ORIGINAL RESEARCH ARTICLE

The photopic negative response of the Light-adapted 3.0 ERG in clinical settings

Gonzalo Ortiz · David Drucker · Connor Hyde · Joseph Staffetti · Jan Kremers ⓘ · Radouil Tzekov ⓘ

Abstract

Purpose   To analyze the effects of different methods of measurement on the photopic negative response (PhNR), recorded as part of a standard ISCEV Photopic 3.0 ERG responses from patients with a variety of clinical diagnoses.

Methods   ERGs were recorded from both eyes of 97 patients (187 eyes) as part of a standard clinical assessment. The average age was 56.4 ± 15.7 years, the gender balance was 35 M, 62F, and only recordable responses of acceptable quality were included. PhNR was measured at an identifiable trough before (PhNR1) and after the i-wave (PhNR2), and the amplitudes and peak times were compared with a-, b- and i-wave corresponding parameters. PhNR compo-nents were measured: from baseline and from b-wave peak. Correlation between PhNR troughs and with ERG parameters were tested for right eyes. The possibility to predict and substitute PhNR2 amplitude from PhNR1 amplitude was also tested.

Results   PhNR1 was recordable in 97.3% of eyes and PhNR2 in 85.6%. An identifiable PhNR2 peak was found to occur before 65 ms at $\sim$ 50% of the records, while in $\sim$ 38% of the cases was within 65–75 ms in $\sim$ 12%—after 75 ms. The correlation between the PhNR1 and PhNR2 peaks was quite strong (with coefficients 0.81–0.98, depending on method of mea-surement, and slopes close to 1). The average differ-ence between predicted and measured PhNR2 was reasonably small in absolute ($< 2 \mu V$) and relative ($< 2\%$) terms. The correlations between PhNR ampli-tudes and other ERG component amplitudes showed different ranges of correlation coefficients depending on the method of measurement: for the a-wave amplitudes the range of coefficients was 0.48–0.73,

Gonzalo Ortiz and David Drucker have contributed equally to this work.

G. Ortiz · D. Drucker · C. Hyde · J. Staffetti · R. Tzekov (✉)
Department of Ophthalmology, University of South Florida, Tampa, FL 33612, USA
e-mail: rtzekov@health.usf.edu

J. Kremers
Department of Ophthalmology, University Hospital Erlangen, Erlangen, Germany

R. Tzekov
Department of Medical Engineering, University of South Florida, Tampa, FL, USA

R. Tzekov
James A. Haley Veterans' Hospital, Tampa, FL, USA

R. Tzekov
The Roskamp Institute, Sarasota, FL, USA

while for the b-wave amplitudes it was 0.30–0.95 and 0.39–0.65 for i-wave.

Conclusion The strong correlation between the two PhNR troughs could allow using PhNR1 when PhNR2 is poorly defined due to artifacts. Different methods of PhNR measurement lead to different correlations with other ERG parameters, and this needs to be considered when analyzing and comparing PhNR data between studies.

Keywords Photopic negative response · Single-flash cone response · Electroretinogram · Retinal disease · ISCEV

Introduction

Electroretinography (ERG) is a recording of a bioelectrical activity of the retina elicited by light stimulation. For clinical purposes, the most widely used type remains the full-field (Ganzfeld) flash ERG, where a brief flash of light (typically 5 ms or less) is presented either in a dark-adapted state or against a photopic background. This type of ERG was standardized first in the late 1980s by the International Society for Clinical Electrophysiology of Vision (ISCEV) [1], with the most recent update of the standard published in 2015 [2]. The ISCEV standard specifies six recording conditions based on the adaptation state of the eye (light- vs. dark-adaptation), the flash intensity and frequency of stimulation. Each condition was created to emphasize specific parameters in order to accentuate their main physiological generator.

Traditionally, the two main ERG components considered to be useful for clinical proposes are the a- and the b-wave. The cellular origin of these two components is relatively well understood. Thus, it is currently generally accepted that the a-wave is generated mostly by photoreceptor activity but carries also some off-bipolar cell contributions that are more prominent under light-adapted conditions [3]. Currently, it is also generally accepted that the b-wave receives a major contribution from on-bipolar cells [4] with contributions from other postreceptoral sources [3].

Under photopic conditions like those specified by the ISCEV standard, two other ERG components can be recorded: an electronegative response following the b-wave peak called the photopic negative response (PhNR), and a positive response superimposed on the PhNR called the i-wave. Although clearly recordable in all normal subjects and most patients, these additional components have not received as much clinical attention as the a- and b-waves and their measurement and reporting have not been standardized, although recently ISCEV published an extended protocol for the PhNR [5].

The cellular origins of the i-wave are a subject of debate and, as such, this component is of uncertain clinical significance. Although early studies suggested that it represents cone off-bipolar cell activity [6], later studies have questioned this origin [7, 8]. Still, even more recent studies seem to suggest at least some relationship between the i-wave and cone off-bipolar cell/cone off-inner retina activity [9–12]. As the i-wave has received very little clinical attention to this day, part of the motivation for the present study was the opportunity to include the i-wave with the traditionally examined ERG components (a- and b-wave) in a clinical sample and under clinically-standardized photopic recording conditions.

The PhNR is an ERG cornea-negative response that occurs after the b-wave and was first reported to receive a significant input from retinal ganglion cell (RGC) activity in monkeys by Viswanathan et al. [13], and this RGC input was later confirmed in humans [14, 15]. Since then, many studies have confirmed the diagnostic potential of PhNR in glaucoma, including early stages and in ocular hypertension [16–26]. Furthermore, reductions in the PhNR amplitude and increase in PhNR peak time were reported in several other ophthalmic and neurologic diseases, including diabetic retinopathy [20, 27–29], optic neuropathy [12, 30], retinal vein occlusion [31–33], childhood optic gliomas [34, 35], elevated intracranial hypertension [36, 37] and multiple sclerosis [38].

The measurement of the PhNR response can be complicated by the relatively slow nature of this potential, where an interference between its course and the i-wave can occur under many recording conditions. Furthermore, ocular movement, including movements similar to the presence of the photomyoclonic reflex [39], which was described under dark-adapted conditions but could occur also under light-adapted condonations (R.T. unpublished data), can

result in uncertainty when determining the precise amplitude of the response.

Although the effort to examine the correlation between PhNR and the other ERG components may seem straightforward at first glance, it is complicated by some factors. For example, under conditions when a white flash on a white background is used to elicit the photopic ERG response, two distinct troughs as part of the PhNR process can appear in relation to the i-wave: one occurring before the i-wave (referred in this work as "PhNR1") and one occurring after the i-wave (referred as "PhNR2") (Fig. 1). While most clinical studies reporting PhNR results have measured and reported PhNR2 amplitude, some studies have measured only PhNR1 amplitude [27, 30, 40]. We are not aware of any studies analyzing both PhNR troughs or how they are related to one another or to the other ERG components. Therefore, we decided to explore the correlations between each trough and the other ERG components and between the troughs themselves.

If a correlation between the PhNR1 and PhNR2 amplitudes is reasonably strong, theoretically it may be possible to predict the PhNR2 amplitude based on PhNR1 amplitude. This would be helpful in cases when determining PhNR2 amplitude may be ambiguous due to interference from blinking or other artifacts. Therefore, we choose to test this possibility using the available data.
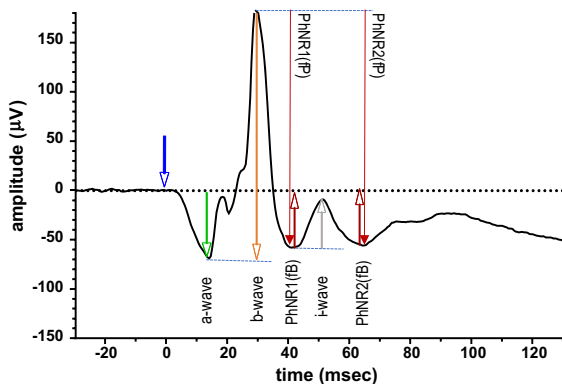

Fig. 1 Example of an ERG waveform recorded under the Photopic 3.0 ERG used in the study for patient #3 (48 years M). Blue arrow indicates the time of the flash. Other arrows indicate peaks of the major ERG components (a-, b-, i-wave and PhNR1 and PhNR2). Both ways of PhNR measurement: from baseline (PhNR1/2(fB)) and from b-wave peak (PhNR1/2(fP)) are illustrated

Currently, there are three ways to determine the amplitude of PhNR [5]. The first and most widely used method is to measure the amplitude from the isoelectric baseline to a minimum point in an identifiable and defined trough, a method to be referred in this work as "from baseline" (fB) (Fig. 1). An alternative approach is to measure from the b-wave peak to the minimum point in an identifiable and defined trough, a method to be referred in this work as "from peak" (fP). One potential disadvantage of this latter method would be an increased dependency on the b-wave amplitude, which has the potential to affect the interpretation of the results in favor of mirroring the effects on the b-wave and artificially suppressing b-wave-independent PhNR changes. Because of artifact-inducing interferences (e.g., blinking), which could prevent a clear determination of a distinct PhNR2 trough, some authors have adopted a third approach, of determining amplitude at a fixed point in time, typically between 65 and 75 ms after flash. To date, very few studies have explored statistical and interpretational implications from using the two major approaches: measurement from baseline to a well-defined trough (fB) or from b-wave peak to a defined trough (fP). Thus, three studies in normal volunteers [41–43] found that the reliability of PhNR amplitude determination is better with the fP method compared to the fB method. To the best of our knowledge, no studies have examined the differences between the two methods measurement in a clinical dataset.

Although it can be predicted that there will be a strong correlation with the b-wave amplitude based on the fP method, the exact degree of correlation in a clinical sample remains unknown. In general, only few studies have examined the correlation between PhNR amplitude and only one ERG parameter, the b-wave, with contradictory results. Thus, Viswanathan et al. [15] found no correlation between PhNR (fB) and the b-wave amplitude in normal healthy volunteers and POAG patients. On the other hand, Mortlock et al. [41] found a significant correlation between the same parameters in normal healthy volunteers. A recent study [44] also showed a significant, relatively strong ($r = 0.76$) correlation between PhNR(fB) and b-wave amplitude in normal healthy volunteers. More importantly, it also demonstrated a relatively weaker ($r = 0.48$), but statistically significant correlation between the same parameters in ABCA4 STGD patients with a significantly different slope, indicating

a potential for a clinical use of the correlation between PhNR and b-wave amplitude in this clinical entity.

Therefore, it would be beneficial to examine to what extent selective changes in the PhNR response may occur and whether they could be correlated with a specific subset of diagnoses in a relatively heterogeneous clinical population. As these changes would manifest as selective changes in PhNR amplitude or timing, independent from changes in other ERG measures, a correlation between PhNR and other ERG measures could demonstrate selectivity and potential for clinical use. This motivated the examination of the influence of the measurement method choice on the degree of correlation between PhNR and other ERG components in a clinical sample as a secondary goal of the present work. We would like to emphasize that the purpose of correlation examinations was not to draw any physiological conclusions, which should be done initially in a normal population, but rather to explore the effect that different ways of measuring PhNR have in a realistic clinically obtained ERG dataset.

Our results show that there is a high degree of correlation between the two PhNR peaks recorded under ISCEV standard Light-adapted 3.0 ERG conditions (PhNR1 and PhNR2), which allows the possibility to use PhNR1 when PhNR2 is poorly defined due to presence of artifacts. Additionally, it was found that different methods of PhNR measurement lead to different correlations with other ERG parameters, and this needs to be considered when analyzing and comparing PhNR data derived by different methods. No selective changes in PhNR were apparent in the current clinical population.

Materials and methods

Patients

This study was a retrospective analysis of the ERG records of patients undergoing routine clinical testing at the USF Eye Institute (Tampa, FL) for the period January 2015–January 2017. Inclusion criteria included: (a) age above 18 years and (b) a recordable Light-adapted 3.0 ERG response with a positive b-wave amplitude greater than 4 μV of acceptable quality.

Electroretinography recordings

The recording was performed binocularly on eyes with dilated pupils (one drop of tropicamide ophthalmic solution 1% and one drop of phenylephrine hydrochloride ophthalmic solution 2.5%) with DTL Plus Electrodes (Diagnosys LLC, Lowell, MA) as active electrodes. Reference electrodes were Ag/AgCl electrodes (Suretrace RTL, ConMed, Utica, NY) placed on the cheekbones with the center of the electrodes vertically aligned with the center of each pupil and positioned at ∼ 1.5 cm below the lower eyelid upper margin, while the ground electrode was the same type as the reference electrode but placed on the left mastoid. The recording system used was UTAS E-3000 (LKC Technologies, Gaithersburg, MD), and the Photopic 3.0 ERG condition as part of a standard clinical setting used white xenon flashes of 3.0 cd s/m^2 on a white background of 30 cd/m^2 after a minimum of 10 min of light adaptation. The band-pass filters were set to 0.1 to 500 Hz, and the sampling rate was 2000 Hz.

Determination of amplitudes and peak times

The a-wave amplitude was measured from baseline to the trough of the first negative response. The b-wave amplitude was measured from the a-wave trough to the peak of the following positive response. The PhNR was measured at two locations on the ERG trace: before the i-wave (PhNR1) and after the i-wave (PhNR2; Fig. 1). A typical ERG waveform under the Light-adapted 3.0 ERG recording condition when both PhNR1 and PhNR2 troughs were clearly identifiable is illustrated in Fig. 1. All recordings were visually inspected, and the presence of both troughs determined by two independent observers. In the case of a disagreement, the appearance of the tracings was discussed and differences resolved.

Statistical analysis

Recordability of the ERG components, defined as presence of a distinct trough determined by two graders, was expressed as percent of all eyes tested for each eye separately and for the aggregated pool of data for both eyes. Normality of the distribution was assessed by D'Agostino–Pearson and Shapiro–Wilk methods. For peak times, skewness and kurtosis of the

distributions were also calculated. An interocular correlation analysis was performed based on Spearman's rank correlation coefficient as most of the datasets did not follow Gaussian distribution. A linear regression was conducted between all recordable ERG components (a-wave, b-wave, PhNR1, i-wave, PhNR2) of right eye recordings. The PhNR amplitudes were measured in two different ways: (a) from baseline (fB) and (b) from the b-wave peak (fP). When performing the regression analysis on amplitudes, outliers were noted, but retained. For peak times in cases of extreme outliers, the analysis was run twice, including and excluding the outliers and the results of both analyses are presented. Wilcoxon matched-pairs signed-ranked test (with Pratt correction when both values identical) was used to compare corresponding amplitudes obtained by peak identification versus by averaged trace and also for comparison between amplitudes of right and left eyes. GraphPad Prism 8.1 (GraphPad Software, La Jolla, CA) was used for graphing and analysis.

Results

Patient demographics

Out of the 155 records evaluated, the records of 94 patients (185 eyes; 33 males and 61 females, average age 56.5 ± 15.6 years, range 19.2 to 80.2 years) passed the inclusion criteria of recordability and were included in the analysis. The identifiers for primary clinical diagnoses of the patients based on the 10th revision of the International Statistical Classification of Diseases and Related Health Problems (ICD-10) were distributed as follows:

- Visual disturbances (H53 or 368)—18 patients
- Blindness and low vision (H54)—10 patients
- Chorioretinal inflammation and other disorders of the choroid (H30/H31)—7 patients
- Other retinal disorders[1] (H35 or 362)—47 patients

---

[1] The H35 is broadly defined category which includes nine distinct subcategories ($n = 38$). The distribution of subcategories and the number of patients within each subcategory were as follows: H35/H53.0 ($n = 4$); H35.1 ($n = 1$), H35.3 ($n = 13$), H35.4 ($n = 3$), H35.5 ($n = 13$), H35.8 ($n = 3$). The full list of all subcategories can be found in [45] and other sources.

- Other categories—12 patients, including: disorders of the ON (H47; $n = 4$); glaucoma (H40; $n = 2$); SCA-7 (G11.8; $n = 2$); disorders of the globe (H44; $n = 2$); other long-term drug therapy (Z79: $n = 1$); benign neoplasm of eye and adnexa (D31; $n = 1$).

Identifiable ERG components and their parameters

Both a- and b-waves were clearly identifiable in all traces that passed the selection criteria used to select the recordings for analysis. On the other hand, while the PhNR1 peak and the i-wave were clearly identifiable in more than 95% of recordings, the PhNR2 trough was identifiable in about 85% of all recordings (Table 1).

A summary of mean amplitudes and peak times for all clearly identifiable ERG components in the current dataset is presented in Table 2. It is worth noting that although recordings were made from patients with either suspected or present retinal degenerations, or other retinal conditions which could lead to a decrease in the ERG photopic response, the mean amplitude values of both a-wave and b-wave were higher compared to the lower limit of normal values used our clinical setting. The lower limits of normal are age dependent and vary between -25 µV for the age range 20–30 years and -18 µV for the oldest age group (70–80 years). For the b-wave, the lower limits were 105 µV for the age range 20–30 years and 85 µV for the age range 70–80 years. A closer look in the amplitude data showed that a large proportion of the a-wave amplitudes, 75% for right eye and 65% for left eye, were within normal range limits, while close to half of the b-wave amplitudes, 50.0% for right eye and 52.7% for left eye, were within normal limits. On the other hand, the average timing of the b-wave was slightly delayed and exceeded the 31 ms, considered to be the upper limit of the normal range; however, only about half of the timings (53.8% for right eye and 47.9% for left eye) turned out to be delayed beyond normal.

PhNR2 peak times

One of the proposed methods to address the uncertainty related to determining a distinct PhNR trough is determining the amplitude at a fixed time period after

Table 1 Recordability of the ERG components in the present study

	a-wave	b-wave	i-wave	PhNR1	PhNR2
Right eye	93	93	88 (95%)	90 (96.8%)	81 (87%)
Left eye	94	94	91 (97%)	92 (97.9%)	79 (84%)
Total	187 (100%)	187 (100%)	179 (96%)	182 (97.3%)	160 (85.6%)

Percent recordability indicated in brackets

Table 2 Mean values and standard deviations of the amplitudes and peak times of the different ERG parameters analyzed in the present study

ERG parameters	Amplitudes (µV)			Peak times (ms)		
	Right eye	Left eye	Average	Right eye	Left eye	Average
a-wave	− 26.3 (12.9)	− 25.9 (12.4)	− 26.2 (11.9)	14.9 (2.8)	14.7 (1.9)	14.8 (2.1)
	n = 93	n = 94	n = 92			
b-wave	93.0 (49.8)	94.8 (47.7)	94.5 (46.3)	32.1 (3.1)	31.9 (3.3)	31.9 (3.1)
	n = 93	n = 94	n = 92			
i-wave	16.7 (12.0)	17.0 (11.0)	16.8 (10.9)	53.7 (6.0)	53.5 (6.0)	53.6 (5.8)
	n = 88	n = 91	n = 87			
PhNR1 (fB)	− 15.4 (15.1)	− 14.9 (13.5)	− 15.2 (13.7)	45.9 (4.3)	45.7 (4.6)	45.8 (4.3)
	n = 90	n = 92	n = 89			
PhNR2 (fB)	− 21.6 (17.2)	− 21.3 (14.8)	− 21.9 (14.9)	66.9 (7.7)	66.9 (8.1)	66.8 (7.7)
	n = 81	n = 79	n = 76			
PhNR1 (fP)	83.5 (36.9)	84.9 (44.6)	84.8 (43.9)	N/A	N/A	N/A
	n = 90	n = 92	n = 89			
PhNR2 (fP)	90.3 (49.7)	94.3 (46.2)	93.4 (45.6)	N/A	N/A	N/A
	n = 81	n = 79	n = 76			

Average values were calculated only when the results from both right and left eyes were present. Abbreviations: fB—PhNR measured from baseline; fP—from b-wave peak; fA|fB—from an averaged amplitude (65–75 ms) to baseline; fA|fP—from an averaged amplitude (65–75 ms) to b-wave peak

the stimulus, often within the interval 65–75 ms. When comparing this method to the method of measurement based on identifying a distinct trough, one of the first questions to answer was how well the time interval of 65 to 75 ms covers the period when identifiable peaks can be found in the current population.

To answer that question, a time analysis was performed on the current sample. The analysis showed that the majority of peak times of identifiable troughs (PhNR2) occurred before 65 ms: 41 cases (51.3%, right eyes) and 38 cases (48.7%, left eyes), compared to 31 cases (38.8%, right eyes) and 30 cases (38.5%, left eyes) in which PhNR2 occurred within the period between 65 and 75 ms. In addition, in 8 (10.0%, right

eyes) and 10 cases (12.8%, left eyes) PhNR2 occurred after 75 ms. Thus, the fact that the mean values of PhNR2 identifiable peak times were within the 65–75 ms period for both right and left eyes (Table 2) appears to underestimate the spread and pattern of peak time distributions in our sample. An additional analysis revealed that the distribution of peak times was non-normal and highly skewed, with levels of skewness of 2.2/2.7 (right/left eyes) and excess kurtosis of 7.8/10.6 (right/left eyes). Such highly skewed distribution would make any assessment of amplitude measured at a fixed time unreliable and unrepresentative for the studied population, and such analysis was not pursued.

Interocular correlations

As tests for normal distribution demonstrated that the parameters in this study when evaluated for right and left eyes separately were not normally distributed, we used Spearman's coefficient to quantify interocular correlations.

The results from the interocular correlation comparison presented in Table 3 demonstrate a high positive correlation (0.7–0.9) for 12 out of the 14 parameters analyzed. However, as correlations varied between different parameters and to avoid complexities related to variability in interocular correlations, only right eyes were used in all subsequent analyses.

Correlation between PhNR1 and PhNR2 amplitudes and peak times

It could be hypothesized the both PhNR troughs (PhNR1, PhNR2) reflect the same retinal mechanism, and therefore, a certain level of high correlation can be expected between the amplitude and timing values of the two troughs. If confirmed, such a correlation would open the possibility to substitute PhNR2 values with PhNR1 values in cases where identifying a distinct PhNR2 trough may be difficult due to the presence of artifacts. To test the validity of that assumption and get an estimate of the degree of correlation, linear regressions were carried between PhNR1 and PhNR2 amplitudes when both troughs were clearly identifiable and also between the corresponding PhNR peak times. The graphical results of the analysis are presented in Fig. 2, while the numerical results are summarized in Table 4. The degree of correlation was

Table 3 Interocular correlations for amplitudes and peak times of all ERG components

	Amplitudes	Peak times
a-wave	0.7953	0.7018
b-wave	0.7968	0.9205
i-wave	0.7830	0.8866
PhNR1 (fB)	0.7919	0.8784
PhNR2 (fB)	0.6607	0.8648
PhNR1 (fP)	0.7822	N/A
PhNR2 (fP)	0.7754	N/A

Values of Spearman's rank correlation coefficient are presented

reasonably high when amplitudes were measured from the isoelectric baseline ($R^2 = 0.82$) and reached strong levels when measured from the b-wave peak ($R^2 = 0.98$). Similarly, the peak times were strongly correlated with each other ($R^2 = 0.87$).

As our population was composed from patients with different presumed or confirmed diagnoses, one concern in examining the correlation between parameters could be the presence of heterogeneity in the clinical sample. In order to assess the effect of the clinical heterogeneity, patient PhNR data presented in Figs. 2, 3, 4 and 5 were color coded into seven diagnostic categories.[2] It is clear from the distribution of the data that no single diagnostic category stands out and data appeared to be relatively homogenous. This impression was confirmed for the other ERG parameters too (see Supplemental Material).

Predictability of PhNR2 amplitude

The possibility to predict and substitute PhNR2 amplitude with PhNR1 amplitude could be useful in cases where the PhNR2 trough is ambiguous. We choose to test this possibility based on PhNR measured by the fP method, as PhNR1(fP) and PhNR2(fP) showed higher correlation level (Table 4). Predictability was tested in two ways. First, a mean conversion coefficient (PhNR2(fP)/PhNR1(fP)) was calculated based on the entire dataset and applied to each PhNR1(fP) value to calculate a predicted PhNR2(fP) value. The results indicating the mean absolute and relative difference between predicted and measured PhNR2(fP) values from both prediction approaches on different groupings of the data are presented in Table 5. They show that the average difference between the predicted and measured PhNR2(fP) was reasonably small in both absolute ($> 2~\mu V$) and relative ($< 2\%$) terms. However, individual differences could reach high values (up to 60%). To examine whether relative individual differences (as % error relative to real amplitude) do have a relationship with PhNR2(fP) amplitude, these values were plotted for right eyes as shown in Fig. 4. It is clear from the data presented in the figure that for most of the data points, the differences were constrained

---

[2] The categories as per ICD-10 classification are as follows: 1) H30 or H31; 2) H35 (or 362); 3) H40; 4) H53 (or 368); 5) H40; 6) H47; 7) other (includes G11.8, H44, Z79 and D31).
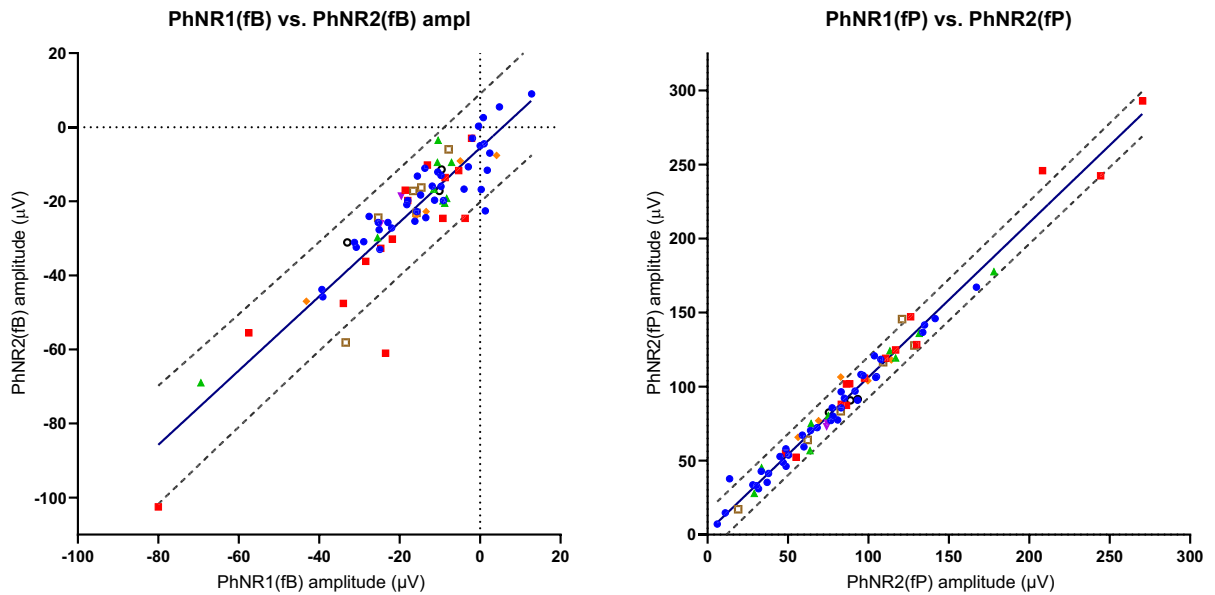
Fig. 2 Correlation between PhNR1 and PhNR2 amplitudes. Left panel, correlation between PhNR1(fB) and PhNR2 (fB); right panel, PhNR1(fP) and PhNR2(fP)

Table 4 Summary of results for linear regression analysis between amplitudes and peak times of PhNR1 and PhNR2

PhNR1 (fB)	PhNR2 (fB)
	0.8191 [0.997]
	(7.4) $n = 79$
PhNR1 (fP)	PhNR2 (fP)
	0.9799 [1.042]
	(7.1) $n = 79$
PhNR1 PT	PhNR2 PT
	0.8732 [1.661]
	(2.8) $n = 79$

Coefficient of determination (R^2) values are presented in bold letters; numbers in square brackets indicate values of slopes, while numbers in round brackets indicate values of standard deviation of the residuals (Sy.x); abbreviations: PT—peak time. In all cases, the slopes of the linear regression models were different from 0 ($p < 0.01$)

Fig. 3 Correlation between PhNR1 and PhNR2 peak times

within ± 15% of real amplitude values and only at amplitudes values lower than 60 μV some differences became bigger. Then, in an alternative approach, a conversion coefficient calculated in the same way was applied on one half of the data and was used to calculate a predicted PhNR2(fP) value in the other half of the data. Similar to the results from the prediction analysis based on the entire dataset, and as expected
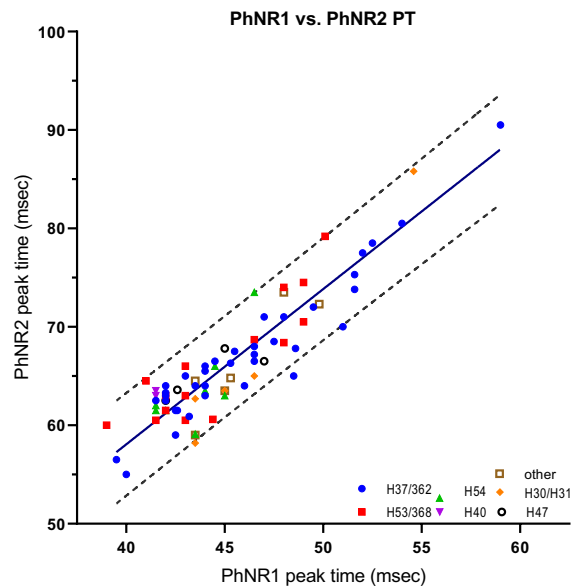
based on using a dataset reduced in half, the difference between the predicted and measured PhNR2(fP) was larger compared to the results from using the whole dataset, but remained relatively small (< 4 μV; < 4%) with individual variation as high as 25%. Similar results were obtained when testing predictability on left eyes (data not shown).
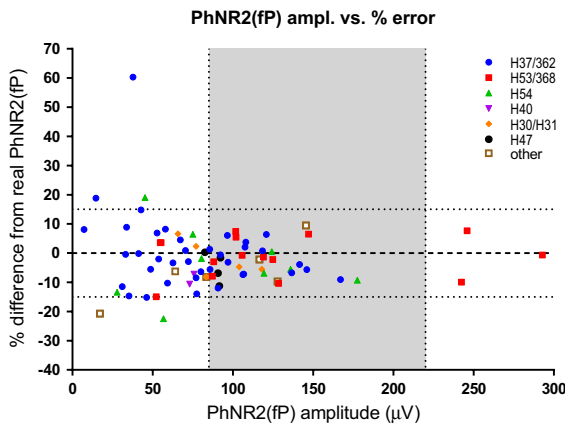
Fig. 4 Relationship between measured PhNR2(fP) amplitude and percent error of PhNR2(fP) amplitude predicted based on a PhNR1(fP) amplitude. The grayed area indicates PhNR2(fP) amplitudes corresponding to a normal b-wave amplitude range

Correlation between PhNR1/b-wave ratio and PhNR2/b-wave ratio

In previous works, the PhNR versus b-wave amplitude ratio has been used as a substitute for PhNR amplitude use in an attempt to improve the discriminatory capability of both b-wave and the PhNR peak in different retinal diseases [17, 23, 41, 46–48]. Therefore, in way similar to the relationship between PhNR1 and PhNR2, it would be useful to examine the relationship between PhNR1/b-wave ratio and PhNR2/b-wave ratio in order to assess whether the PhNR2/b-wave ratio could be substituted by the PhNR1/b-wave ratio when the PhNR2 trough is difficult to define. The results of exploring the relationships between PhNR1/b-wave and PhNR2/b-

wave ratios derived in different ways based on the type of measured used to determine PhNR are presented in Fig. 5 and Table 6. The results demonstrated that the relationships between the ratios were considerably lower compared to the relationships between PhNR amplitudes. Thus, $R^2 = 0.24$ for the ratios versus $R^2 = 0.98$ for the amplitudes (fP method) and $R^2 = 0.41$ for the ratios versus $R^2 = 0.82$ for the amplitudes (fB method).

Correlation between PhNR and other ERG components' amplitudes

First, we explored the correlations between PhNR amplitudes measured from baseline and the other major ERG components (a-, b- and i-wave). The graphical representation of the linear regressions between the PhNR1(fB) and PhNR2(fB) on one hand and a-, b- and i-wave amplitudes on the other hand is shown in Supplemental Fig. 1, while the numerical results are summarized in Supplemental Table 1. The correlation between PhNR1 and PhNR2, when measured from the bioelectrical baseline, appears to be slightly stronger with the a-wave amplitude (R^2 range 0.48–0.51), compared to the correlation with both b-wave ($R^2 = 0.30$–0.43) and i-wave amplitude ($R^2 = 0.39$–0.41).

We next explored the linear relationship between the amplitudes of PhNR measurements from the preceding b-wave peak (PhNR1(fP) and PhNR2(fP)) and the amplitudes of the main ERG components (a, b- and i-wave) (Supplemental Fig. 1, Supplemental Table 1). The correlation of the PhNR1(fP) and

Table 5 Testing predictability of PhNR2(fP) values based on PhNR1(fP) values

	A. Based on whole dataset			B. Based on the 1st half of the data		
	Mean difference with real PhNR2 (µV)	Mean difference with real PhNR2 (%)			Mean difference with real PhNR2 (µV)	Mean difference with real PhNR2 (%)
Average	− 1.99	− 1.6	Average	− 3.65	− 3.8
SD	7.43	10.8	SD	6.72	8.9
n	79	79	*n*	39	39
min	− 24.09	− 22.5	min	− 19.87	− 24.6
max	22.71	60.3	max	11.50	17.4

The mean difference between predicted and real values for PhNR2(fP) is shown for right eyes and the two methods used: (A) for the whole dataset, based on a coefficient derived from the whole dataset; (B) for the second half of the data based on a coefficient derived from the first half of the data. For more detail, see main text
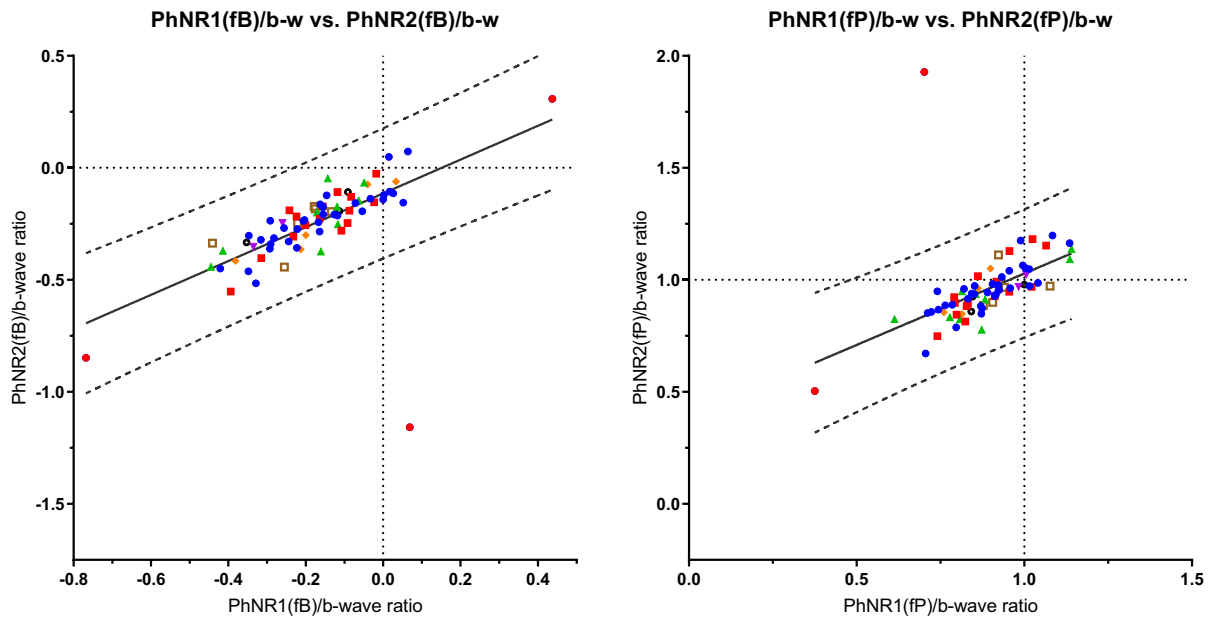
PhNR1(fB)/b-w vs. PhNR2(fB)/b-w

PhNR1(fP)/b-w vs. PhNR2(fP)/b-w

Fig. 5 Correlation between PhNR1/b-wave and PhNR2/b-wave ratios. Left panel represents correlations between PhNR1(fB)/b-wave ratio versus PhNR2(fB)/b-wave ratio; right

panel represents correlations between PhNR1(fP)/b-wave ratio versus PhNR2(fP)/b-wave ratio. Symbols in red color indicate outliers

Table 6 Summary of results for linear regression analysis between of PhNR1/b-wave and PhNR2/b-wave ratios

PhNR1(fB)/b-wave	PhNR2(fB)/b-wave
	0.4148 [0.7547]
	(0.144); $n = 79$
PhNR1(fP)/b-wave	PhNR2(fP)/b-wave
	0.2445 [0.6379]
	(0.142); $n = 79$

Coefficient of determination (R^2) values are presented in bold letters; numbers in square brackets indicate slope of the linear regression; numbers in round brackets indicate values of standard deviation of the residuals (Sy.x). In all cases, the slopes of the linear regression models were different from 0 ($p < 0.01$)

PhNR2(fP) with a-wave amplitude increased noticeably compared to the same range when PhNR amplitudes were measured from baseline (0.73–0.74 vs. 0.48–0.51). Furthermore, the correlation with b-wave amplitude increased dramatically (0.94–0.95 vs. 0.30–0.43), as can be expected because of the inclusion of the b-wave in the fP measurements. The correlation of PhNR peaks with the i-wave amplitude also increased substantially (0.65 vs. 0.39–0.41), perhaps because of the use of the peak-to-trough

method as opposed to peak to baseline method as in fB.

Correlation between PhNR and main ERG parameters peak times

Next, the correlation between the peak times of the PhNRs in cases when troughs were clearly identifiable and the peak times of major ERG components (a, b- and i-wave) was studied. The graphical results are shown in Supplemental Fig. 2, while the numeric results are presented in Supplemental Table 2. In a preliminary run of the analysis, it appeared that a-wave peak times contained a few outliers, which influenced the slope of the linear regression (Supplemental Fig. 2 top left panel). Therefore, in the analysis, the correlation was explored twice: once with the outliers present (Supplemental Fig. 2 top left panel), and once with all a-wave peak times occurring later than 20 ms post-stimulus removed (Supplemental Fig. 2 bottom left panel). The second approach resulted in a considerable improvement of the coefficients of determination and reduction of standard deviation of the residuals (Supplemental Table 2).

Overall, the correlations between the peak times of the PhNRs and the peak times of the main ERG

components ranked as expected, based on temporal proximity between the peaks: the correlation was strongest with the i-wave peak time (0.84–0.89), followed by the b-wave peak time (0.72–0.79) and weakest with the a-wave peak time (0.50–0.58; with outliers removed).

Discussion

Despite the recent publication of an ISCEV extended protocol for the photopic negative response (PhNR) of the full-field electroretinogram [5], there are still challenges hampering the standardization of the PhNR recording and measurement. For example, occurrence of the photomyoclonic reflex or blinking could interfere with the determination of the PhNR peak. Similarly, the timing of the i-wave (or, occasionally, the appearance of more than one i-wave) could coincide and interfere with the determination of a single distinct PhNR trough. Furthermore, different combinations of stimulus conditions (wavelength composition and intensity of the stimulus or the background) could stimulate different subpopulations of retinal ganglion cells, which can be differentially affected in different retinal conditions. While we agree with the recommendation of the ISCEV extended protocol [5] that it may be preferable to record the PhNR using red flash on a rod-saturating blue background, in this work, we explored the relationship between the PhNR responses generated by standard clinical recording conditions as in Light-adapted 3.0 ERG [2]. As this type of response has been a part of the ISCEV standard for the last 30 years [1], it provides the advantage that data can be analyzed retrospectively and recorded with older ERG systems, which lack the capability of providing narrowband wavelength stimulation.

Under the conditions of recording used in the present work, in the vast majority of the cases, and as shown on Fig. 1, the i-wave was occurring at the time of a projected maximum negativity after the b-wave, where an assumed single PhNR trough would be present if i-wave was non-existent. Because of i-wave interference, two distinct troughs appeared, one occurring before the i-wave (PhNR1) and one after it (PhNR2). While most studies have used PhNR2, some studies have assigned and measured the PhNR1 trough [27, 30, 40, 49], or choosing the PhNR1 or PhNR2,

depending which one was more negative [42]. Therefore, we decided to analyze both peaks and their relationships with the rest of the ERG components and between themselves.

Interchangeability between PhNR1 and PhNR2 amplitudes

As mentioned in introduction, various authors have found it difficult to determine a reliable location and identification of the PhNR2 peak in all cases. This has been also our experience in the present study, where we were unable to reliably determine the PhNR2 peak in $\sim$ 12% of recordings where the PhNR1 trough was clearly identifiable (Table 1). Therefore, an important question is whether the PhNR1 amplitude could be used as a surrogate for PhNR2 amplitude determination (with a correction factor) in these cases. If both troughs are part of the same process, it could be assumed that they are correlated with each other and some degree of equivalence should be present. Based on the analysis of the dataset in the present study, it appears that such a correlation is present and reaches strong levels when using the fP measurement approach (0.98). This is supported by the relatively strong correlation by the PhNR1 and PhNR2 peak times (0.87), which are independent from the method of amplitude measurement. Our additional analysis of predictability based on PhNR1(fP) amplitude shows that at a group level the prediction can be successful and relatively very accurate with an average error of less than 5%. However, such prediction would have a much more variable rate of success on an individual level, especially for PhNR2 amplitudes of < 60 µV. In general, these findings support the possibility of interchangeable use of the two parameters at a group level under recording conditions similar to the ones presented in this study. This could further enhance the diagnostic usability of PhNR and outweigh a minor drawback, which is the need to obtain normative values for both peaks.

As an extension of this approach, theoretically one could also suggest substituting the PhNR2/b-wave amplitude ratio with PhNR1/b-wave amplitude ratio under similar circumstances. Yet the predictability test based on data from our clinical sample showed that such substitution, even at a group level, would be much less accurate and the results much more variable. This is probably due to different sources of

variability for b-wave and PhNR and their possible non-linear interference.

Measurement at fixed time versus at identifiable peak

The extended ISCEV protocol for PhNR recording outlines the possibility for measuring the PhNR amplitude based on a choice of fixed time in the ERG trace occurring between within the interval 65 and 75 ms after stimulus [5]. However, in our dataset, the majority of identifiable troughs occurred before this time interval and some occurred after (see Results). The most likely explanation for this discrepancy lies in the characteristics of the stimulation in the present study (white xenon flash on a white background versus red stimulus on a blue background as recommended in [5]). Of note, a study by Bhatti et al. [50] found differences in heritability and effects of age between PhNR amplitude determined by identifying a distinct PhNR trough versus amplitudes measured at a fixed time (65 ms) by the fB method under stimulus conditions similar to ours. Thus, caution should be taken with the implementation and interpretation of results obtained by the fixed time method, especially when analyzing recordings of Light-adapted 3.0 ERG for changes in PhNR.

Measurement from baseline versus from b-wave peak and using PhNR to b-wave ratio

The two alternative ways of PhNR amplitude measurement: from the isoelectrical baseline (fB) and from the b-wave peak (fP) have each advantages and disadvantages. The amplitude measured from baseline is easier to visualize and this could lead to more intuitive interpretation of the results. On the other hand, due to the nature of the measurement, the measurement from the b-wave peak results in larger and positive values, which makes it easier to assess relative differences between amplitudes, especially in records where amplitudes measured by the fB method are smaller and become closer to (or slightly elevated above) the isoelectric baseline. At the same time, as stated in the extended ISCEV protocol [5], it has to be noted that the (fP) approach results in a response with an enhanced correlation with the b-wave, which has to be taken into account when interpreting the results. The data obtained in the present study reveal

additional differences between the two methods. First, although the correlation with b-wave was indeed substantially stronger with the (fP) compared to the (fB) method, the PhNR correlation with both a- and i-wave increased in a similar manner, but to a lesser extent as compared to the increase in correlation between PhNR(fB) versus PhNR(fP) and the b-wave (Supplemental Table 1).This it be expected, as PhNR(fP) is strongly correlated to the b-wave, while it is less correlation to both a- and i-wave.

Study limitations

The main limitation of the present study related to the fact that the study population was composed only by patients and may have limited applicability to normal subjects. However, it has to be kept in mind that, the majority of the patients were only suspected to have retinal degenerative disease process, which may have or may have not been confirmed with further testing. This is further supported by the finding that $\sim 47\%$–70% of the a- and b-wave amplitude values and $\sim 50\%$ of b-wave peak times were within normal limits. In any case, our main goal was to explore changes and relationships between the ERG components within a typical patient population and any implication regarding normal subjects would carry only a secondary significance.

Conclusion

This study demonstrated that in a diverse patient population sample, the standard Light-adapted 3.0 ERG response (single-flash cone ERG in ISCEV standard before 2005) generated a PhNR waveform that was recordable and had more than 85% identifiable and measurable PhNR troughs. The analysis carried by this study indicates that the uncertainty related to determination of the PhNR peak after the i-wave can be circumvented by measuring the peak preceding the i-wave. It also reveals complex relationships between PhNR and the other ERG components and shows that the method of PhNR amplitude measurement can have a substantial impact on the relationship between PhNR and other ERG parameters. Thus, caution is needed when comparing PhNR amplitude results derived from different methods of measurement. These findings support the notion that

PhNR could be used clinically in a reliable manner to estimate the function of the retinal ganglion cells in a variety of ophthalmic and neurologic conditions.

References

1. Marmor MF, Arden GB, Nilsson SEG, Zrenner E (1989) Standard for clinical electroretinography. International Standardization Committee. Arch Ophthalmol 107(6):816–819

2. McCulloch DL et al (2015) ISCEV standard for full-field clinical electroretinography (2015 update). Doc Ophthalmol 130(1):1–12

3. Sieving PA, Murayama K, Naarendorp F (1994) Push-pull model of the primate photopic electroretinogram: a role for hyperpolarizing neurons in shaping the b-wave. Vis Neurosci 11(3):519–532

4. Stockton RA, Slaughter MM (1989) B-wave of the electroretinogram: a reflection of ON bipolar cell activity. J Gen Physiol 93(1):101–122

5. Frishman L et al (2018) ISCEV extended protocol for the photopic negative response (PhNR) of the full-field electroretinogram. Doc Ophthalmol 136(3):207–211

6. Nagata M (1963) Studies on the photopic ERG of the human retina. Jpn J Ophthalmol 7:96–124

7. Seiple W, Holopigian K (1993) The 'OFF' response of the human electroretinogram does not contribute to the brief flash 'b-wave'. Vis Neurosci 11:667–673

8. Rousseau S, McKerral M, Lachapelle P (1996) The i-wave: bridging flash and pattern electroretinography. Electroencephalogr Clin Neurophysiol Suppl 46:165–171

9. Rufiange M et al (2002) Cone-dominated ERG luminance-response function: the Photopic Hill revisited. Doc Ophthalmol 104(3):231–248

10. Lachapelle P et al (1998) Evidence supportive of a functional discrimination between photopic oscillatory potentials as revealed with cone and rod mediated retinopathies. Doc Ophthalmol 95(1):35–54

11. Rosolen SG et al (2004) Comparing the photopic ERG i-wave in different species. Vet Ophthalmol 7(3):189–192

12. Rangaswamy NV et al (2004) Photopic ERGs in patients with optic neuropathies: comparison with primate ERGs after pharmacologic blockade of inner retina. Invest Ophthalmol Vis Sci 45(10):3827–3837

13. Viswanathan S et al (1999) The photopic negative response of the macaque electroretinogram: reduction by experimental glaucoma. Invest Ophthalmol Vis Sci 40(6):1124–1136

14. Colotto A et al (2000) Photopic negative response of the human ERG: losses associated with glaucomatous damage. Invest Ophthalmol Vis Sci 41(8):2205–2211

15. Viswanathan S et al (2001) The photopic negative response of the flash electroretinogram in primary open angle glaucoma. Invest Ophthalmol Vis Sci 42(2):514–522

16. Wakili N et al (2008) The photopic negative response of the blue-on-yellow flash-electroretinogram in glaucomas and normal subjects. Doc Ophthalmol 117(2):147–154

17. Machida S et al (2008) Correlation between photopic negative response and retinal nerve fiber layer thickness and optic disc topography in glaucomatous eyes. Invest Ophthalmol Vis Sci 49(5):2201–2207

18. Sustar M, Cvenkel B, Brecelj J (2009) The effect of broadband and monochromatic stimuli on the photopic negative response of the electroretinogram in normal subjects and in open-angle glaucoma patients. Doc Ophthalmol 118(3):167–177

19. North RV et al (2010) Electrophysiological evidence of early functional damage in glaucoma and ocular hypertension. Invest Ophthalmol Vis Sci 51(2):1216–1222

20. Kim HD, Park JY, Ohn YH (2010) Clinical applications of photopic negative response (PhNR) for the treatment of glaucoma and diabetic retinopathy. Korean J Ophthalmol 24(2):89–95

21. Kremers J et al (2012) Spectral characteristics of the PhNR in the full-field flash electroretinogram of normals and glaucoma patients. Doc Ophthalmol 124(2):79–90

22. Huang L et al (2012) Clinical application of photopic negative response of the flash electroretinogram in primary open-angle Glaucoma. Eye Sci 27(3):113–118

23. Preiser D et al (2013) Photopic negative response versus pattern electroretinogram in early glaucoma. Invest Ophthalmol Vis Sci 54(2):1182–1191

24. Niyadurupola N et al (2013) Intraocular pressure lowering is associated with an increase in the photopic negative response (PhNR) amplitude in glaucoma and ocular hypertensive eyes. Invest Ophthalmol Vis Sci 54(3):1913–1919

25. Kirkiewicz M, Lubinski W, Penkala K (2016) Photopic negative response of full-field electroretinography in patients with different stages of glaucomatous optic neuropathy. Doc Ophthalmol 132(1):57–65

26. Cvenkel B, Sustar M, Perovsek D (2017) Ganglion cell loss in early glaucoma, as assessed by photopic negative response, pattern electroretinogram, and spectral-domain optical coherence tomography. Doc Ophthalmol 135(1):17–28

27. Kizawa J et al (2006) Changes of oscillatory potentials and photopic negative response in patients with early diabetic retinopathy. Jpn J Ophthalmol 50(4):367–373

28. Chen H et al (2008) The photopic negative response of flash ERG in nonproliferative diabetic retinopathy. Doc Ophthalmol 117(2):129–135

29. McFarlane M et al (2012) Blue flash ERG PhNR changes associated with poor long-term glycemic control in adolescents with type 1 diabetes. Invest Ophthalmol Vis Sci 53(2):741–748

30. Gotoh Y, Machida S, Tazawa Y (2004) Selective loss of the photopic negative response in patients with optic nerve atrophy. Arch Ophthalmol 122(3):341–346

31. Chen H et al (2006) The photopic negative response of the flash electroretinogram in retinal vein occlusion. Doc Ophthalmol 113(1):53–59

32. Moon CH et al (2013) Visual prognostic value of photopic negative response and optical coherence tomography in central retinal vein occlusion after anti-VEGF treatment. Doc Ophthalmol 126(3):211–219

33. Gardasevic Topcic I et al (2014) Morphological and electrophysiological outcome in prospective intravitreal bevacizumab treatment of macular edema secondary to central retinal vein occlusion. Doc Ophthalmol 129(1):27–38

34. Abed E et al (2015) Functional loss of the inner retina in childhood optic gliomas detected by photopic negative response. Invest Ophthalmol Vis Sci 56(4):2469–2474

35. Falsini B et al (2016) Nerve growth factor improves visual loss in childhood optic gliomas: a randomized, double-blind, phase II clinical trial. Brain 139(Pt 2):404–414

36. Moss HE, Park JC, McAnany JJ (2015) The photopic negative response in idiopathic intracranial hypertension. Invest Ophthalmol Vis Sci 56(6):3709–3714

37. Park JC, Moss HE, McAnany JJ (2018) Electroretinography in idiopathic intracranial hypertension: comparison of the pattern ERG and the photopic negative response. Doc Ophthalmol 136(1):45–55

38. Wang J et al (2012) The photopic negative response of the flash electroretinogram in multiple sclerosis. Invest Ophthalmol Vis Sci 53(3):1315–1323

39. Johnson MA, Massof RW (1982) The photomyoclonic reflex: an artefact in the clinical electroretinogram. Br J Ophthalmol 66(6):368–378

40. Thompson DA et al (2011) Altered electroretinograms in patients with KCNJ10 mutations and EAST syndrome. J Physiol 589(Pt 7):1681–1689

41. Mortlock KE et al (2010) Inter-subject, inter-ocular and inter-session repeatability of the photopic negative response of the electroretinogram recorded using DTL and skin electrodes. Doc Ophthalmol 121(2):123–134

42. Binns AM, Mortlock KE, North RV (2011) The relationship between stimulus intensity and response amplitude for the photopic negative response of the flash electroretinogram. Doc Ophthalmol 122(1):39–52

43. Tang J et al (2014) The test–retest reliability of the photopic negative response (PhNR). Transl Vis Sci Technol 3(6):1

44. Abed E et al (2018) Early impairment of the full-field photopic negative response in patients with Stargardt disease and pathogenic variants of the ABCA4 gene. Clin Exp Ophthalmol 46(5):519–530

45. Reference, I.-.-C.P.M.C. ICD10Data. 2018 [cited 2018 9/22/2018]; 2018 ICD-10-CM/PCS Medical Coding Reference]. Available from: https://www.icd10data.com/

46. Gowrisankaran S et al (2011) Structural and functional measures of inner retinal integrity following visual acuity improvement in a patient with hereditary motor and sensory neuropathy type VI. Ophthalmic Genet 32(3):188–192

47. Moon CH et al (2011) The time course of visual field recovery and changes of retinal ganglion cells after optic chiasmal decompression. Invest Ophthalmol Vis Sci 52(11):7966–7973

48. Wu Z et al (2016) Measuring the photopic negative response: viability of skin electrodes and variability across disease severities in glaucoma. Transl Vis Sci Technol 5(2):13

49. Miyata K et al (2007) Reduction of oscillatory potentials and photopic negative response in patients with autosomal dominant optic atrophy with OPA1 mutations. Invest Ophthalmol Vis Sci 48(2):820–824

50. Bhatti T et al (2017) Relative genetic and environmental contributions to variations in human retinal electrical responses quantified in a twin study. Ophthalmology 124(8):1175–1185